Department of Pharmacy, Union Hospital, Tongji Medical College, Huazhong University of Science and Technology, Wuhan, China

Effects of aprepitant on the pharmacokinetics of imatinib and its main metabolite in rats

Sanaz Darbalaei#, Xinlin Zhang, Nanxi Wang, Yanjie Qin, Xuemei Han, Ying Rang, Xuejia Zhai*, Yongning Lu*

Received December 20, 2017, accepted January 19, 2018

**Corresponding authors: Yongning Lu, Xuejia Zhai, Department of Pharmacy, Union Hospital, Tongji Medical College, Huazhong University of Science and Technology, No. 1277, Jiefang Avenue, Wuhan 430022, Hubei Province, China*
luyn_union@163.com
 # co-first author

Pharmazie 73: 329–334 (2018) *doi: 10.1691/ph.2018.7335*

Aprepitant (APT), an antiemetic drug belonging to the class of substance P antagonists is efficiently used in both acute and delayed chemotherapy-induced nausea and vomiting. Nausea and vomiting induced by imatinib (IMA) as a chemotherapeutic drug could be reduced by APT. This study investigated the effect of APT on the pharmacokinetics of IMA and its major metabolite N-desmethyl imatinib (N-D IMA) in rats and the mechanism of this drug-drug interaction. The results indicated that after 3 days of pretreatment with APT (10 mg/kg), the blood concentration of IMA was decreased in both of oral and intravenous routes of IMA administration compared to vehicle treated rats, whereas the blood concentration of N-D IMA was not significantly changed. The total clearance (CL/F) of oral and intravenous given IMA was increased by 1.41 and 1.32-fold, and the bioavailability was greatly decreased about 30.43% and 24.40% respectively. At this time, the P-gp and the hepatic CYP3A1 were increased at both the mRNA and protein levels. These results demonstrated that ingestion of APT will decrease the bioavailability of IMA to a significant extent in rats and the drug-drug interaction between APT and IMA appears to be due to modulation of P-gp and CYP3A1.

1. Introduction

Imatinib (IMA), a selective anticancer drug is recently undergoing broader consideration due to its activity against chronic myeloid leukemia (CML) and gastrointestinal stromal tumors (GIST) (Gotta et al. 2014; George and Trent 2011; Zitvogel et al. 2016). An unique combination of biological, pharmacokinetic and pharmacogenomic factors such as genetic polymorphisms along with the mechanisms for controlling each cytochrome P450 (CYP) 3A4 expression are criteria for different exposure amounts of IMA among the patients (Scripture et al. 2005). IMA is rapidly and completely absorbed with an oral bioavailability of exceeding 90 % (Delbaldo et al. 2006). Upon reaching the liver, IMA is predominantly metabolized (80%) to its major circulating metabolite N-D IMA by CYP3A4 and 2C8-mediated N-demethylation in humans (Khan et al. 2016; Takahashi and Miura 2012). CYP3A5, CYP1A1, CYP1A2, CYP2D6, CYP2C9 and CYP2C19 play little or no role (Rochat et al. 2010; Filppula et al. 2013). N-D IMA was reported to have the same intrinsic affinity as the plasma drug level of the parent compound with longer half-life although with three to four times lower pharmacological activity (Takahashi and Miura 2012; Egerer et al. 2010). By retrospective look at previous studies, IMA and N-D IMA are substrates of P-glycoprotein (P-gp/ABCB1) and breast cancer resistance protein (BCRP/ABCG2) transporters. Thus, it is important to quantify IMA and its metabolite concentrations in plasma and evaluate their pharmacokinetic profiles for successful drug-drug interaction management.

Nausea and vomiting are the most common distressing side-effects of chemotherapy. APT, an orally available, selective neurokinin-1 receptor antagonist is effective in combination with a 5-hydroxytryptamine-3 antagonists and a corticosteroid for treatment of moderately and highly emetogenic chemotherapy (Huskey et al. 2004). APT plays an important clinical role in eliminating nausea and vomiting caused by IMA administration.

Interactions based on metabolism have been increasingly reported between drug and drug or diet (Prueksaritanont et al. 2013). By considering the APT history, it was reported to be a moderate inhibitor of CYP3A4 and increased the AUC of oxycodone by 25% and also enhanced midazolam, methylprednisolone and dexamethasone bioavailabilities (Majumdar et al. 2003; Fujiwara et al. 2014), while other studies have shown induction of this enzyme by APT (Shadle et al. 2004). It is also declared to have transient induction on CYP2C9 in pharmacokinetic studies of some drugs such as tolbutamide, warfarin and diclofenac (NSAIDs) (Depré et al. 2005; Aapro and Walko 2010). Moreover, *in vitro* data have shoen that APT exhibited a weak inhibitory effect on Pgp transporter (Feuring et al. 2003). Interactions may occur when APT is co-administered with drugs which are substrates of either of these enzymes or transporters.

APT might have the potential to modulate plasma IMA and N-D IMA levels as they have mutual metabolic enzymes and transporters (Egerer et al. 2010). In this study, we investigated the effects of APT on the pharmacokinetics of IMA and N-D IMA, simultaneously detected by LC–MS/MS method in rat plasma.

2. Investigations and results

2.1. LC–MS/MS analysis

The retention times for IMA, N-D IMA and gefitinb were 2.18, 2.06 and 1.31 min, respectively as represented in Fig. 1a (free plasma), 1b (plasma spiked with lower limit of quantification (LLOQ), and 1c (plasma spiked with IMA samples). Calibration curves were linear over the ranges of 0.05 to 150 µg/mL for IMA and 0.025 to 5.0 µg/mL for N-D IMA. The LLOQ concentrations were 0.05 µg/mL and 0.025 µg/mL for IMA and N-D IMA, respectively. All data were in the accuracy range of 95.37 – 111.45%. The relative standard deviation (RSD) of precision was likewise acceptable (between 3.29 and 5.70 % for IMA; between 1.34 and 8.83 % for N-D IMA). The extract recovery of all analytes, determined at LLOQ and three quality control samples at low, medium and high levels (QCL, QCM and QCH), was greater than 89.34

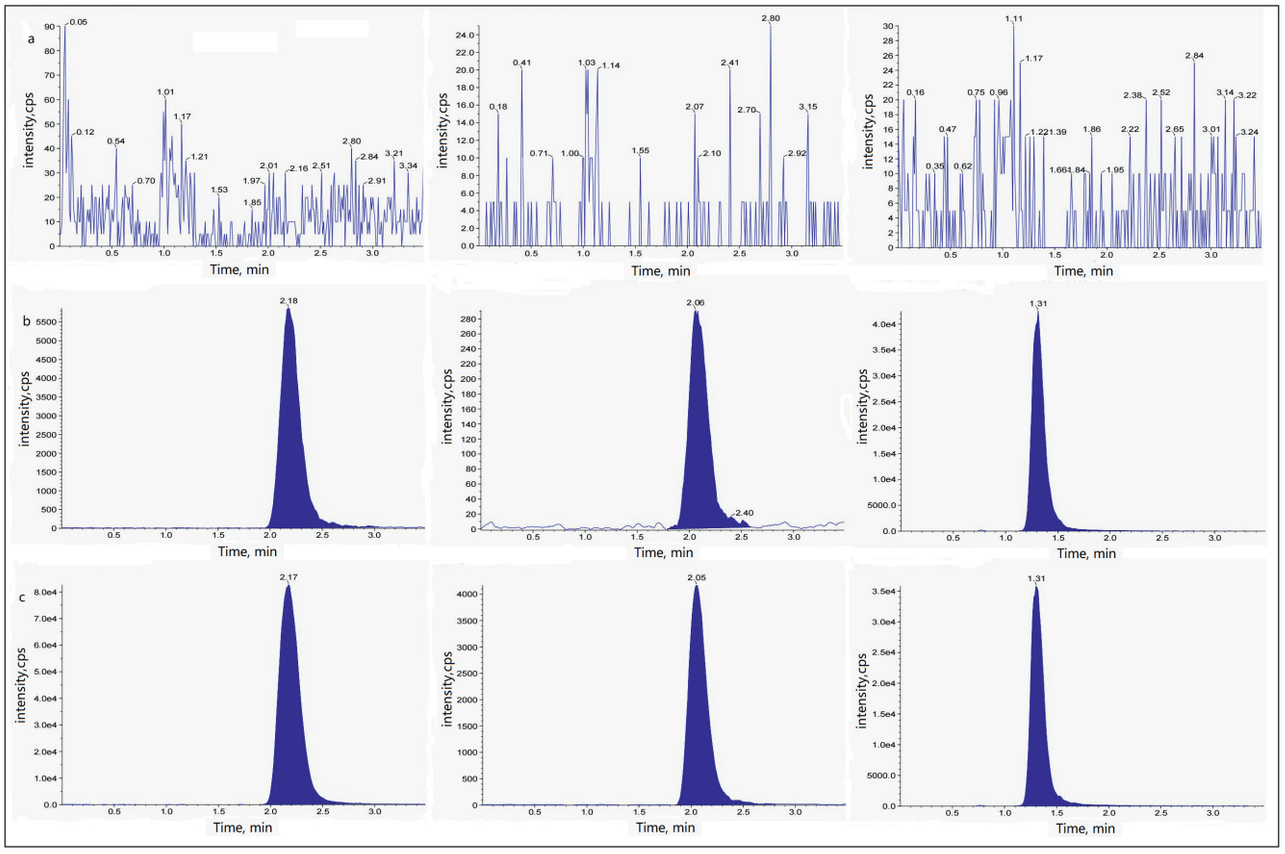

Fig. 1: Representative chromatograms of rats free plasma (a); spiked plasma with relative LLOQ (b); and IMA treated plasma (c) samples

%. Stability of the samples under the assay conditions was secure. The above results demonstrated that there was no endogenous substance influenced by ion suppression, the values were within the acceptable range and the method was accurate and precise.

2.2. *Pharmacokinetic study in rats*

To understand the target and the extent of interaction between APT and IMA, IMA was administered by oral and intravenous routes separately. As shown in Fig. 2, a and b, IMA was given orally to the rats with different pretreatments over 3 days. The pharmacokinetic data of IMA and N-D IMA for different groups are listed in Table 1. A CYP3A4 inducer (dexamethasone) significantly decreased the bioavailability of IMA by 3.8-fold lowering of the AUC, reducing C_{max} by 2.7-fold *(P*<0.05) and increasing AUC and Cmax of N-D IMA by 1.40 and 1.58-fold (P<0.05). After pre-administration of the CYP3A4 inhibitor ketoconazole, the AUC was greatly increased for IMA (P<0.05) and decreased for N-D IMA (P<0.01). Ketoconazole significantly downregulated CL/F and V/F levels of IMA and upregulated them for this metabolite, the Cmax of IMA was slightly decreased compared with the control.

When IMA was administered intravenously, as shown in Fig. 2, c and d and Table 2, AUC and MRT decreased by 1.81 and 1.50-fold for IMA, respectively. They were increased by 1.64 and 1.06-fold for N-D IMA in the group pretreated with the CYP3A4 inducer. On the contrary, the CYP3A4 inhibitor ketoconazole significantly increased the bioavailability of IMA and decreased that of N-D IMA.

After three days of APT treatment, the AUC of the oral and intravenous IMA were significantly (P<0.05) decreased about 30.43% and 24.40% relatively versus the control group. Additionally Cmax was decreased about 11.0% in orally given IMA. The CL/F was significantly increased to 0.73±0.09 L/h/kg and 6.68±1.30 L/h/kg (P<0.05). However, N-D IMA plasma concentration and pharmacokinetic parameters were not significantly changed compared to the corresponding controls in both oral and intravenous routes.

Table 1: Pharmacokinetic parameters of IAM and N-D IMA after oral administration of IMA (30 mg/kg) to the pretreated groups given oral 0.5% CMC-Na, ketoconazole (80 mg/kg) , dexamethasoneand (80 mg/kg) and APT (10 mg/kg) to rats for 3 consecutive days (n = 6)

Parameter	*Control*	*APT*	*Ketoconazole*	*Dexamethasone*
IMA				
$AUC_{0\text{-}t}$(mg·h·L^{-1})	59.93±10.09	41.76±4.68**	77.66±11.30*	15.66±5.20**
$AUC_{0\text{-}\infty}$(mg·h·mL^{-1})	60.05±10.15	41.77±4.68**	79.24±8.83*	16.19±4.65**
C_{max}(mg/L)	7125.0±2040.3	6343.3±681.0	6165.0±1247.9	2647.2±1601.3**
T_{max}(h)	2.67±0.74	2.0±0.63	1.8±0.64	1.7±0.52
$T_{1/2}$(h)	3.57±0.74	2.99±0.16	5.38±1.24*	2.27±1.23
Vd/F(L·kg^{-1})	2.62±0.63	3.14±0.38	3.79±1.95	6.02±1.64*
CL/F(L·h^{-1}·kg^{-1})	0.51±0.10	0.73±0.09*	0.37±0.11*	1.99±0.61**
N-D IMA				
$AUC_{0\text{-}t}$(mg·h·L^{-1})	2.60±0.67	2.03±0.46	0.61±0.30*	3.63±1.34*
$AUC_{0\text{-}\infty}$(mg·h·mL^{-1})	2.60±0.67	2.05±0.47	0.65±0.34*	3.66±1.34*
C_{max}(mg/L)	259.8±66.3	242.8±58.2	36.4±20.9*	410.2±264.0*
T_{max}(h)	3.52±1.38	4.31±1.51	4.01±1.35	4.22±1.12
$t_{1/2}$(h)	4.26±0.67	5.56±1.35	5.17±1.76	5.13±1.52
Vd/F(L·kg^{-1})	75.9±32.5	119.8±36.7	541.4±287.6*	66.6±27.6
CL/F(L·h^{-1}·kg^{-1})	12.22±3.35	15.28±3.27	57.61±27.21	9.05±2.92

Each value represents the mean ± S.D. of six rats.
* Significantly different with P < 0.05 versus 0.5% CMC-Na (control group).
** Significantly different with P < 0.01 versus 0.5% CMC-Na (control group).

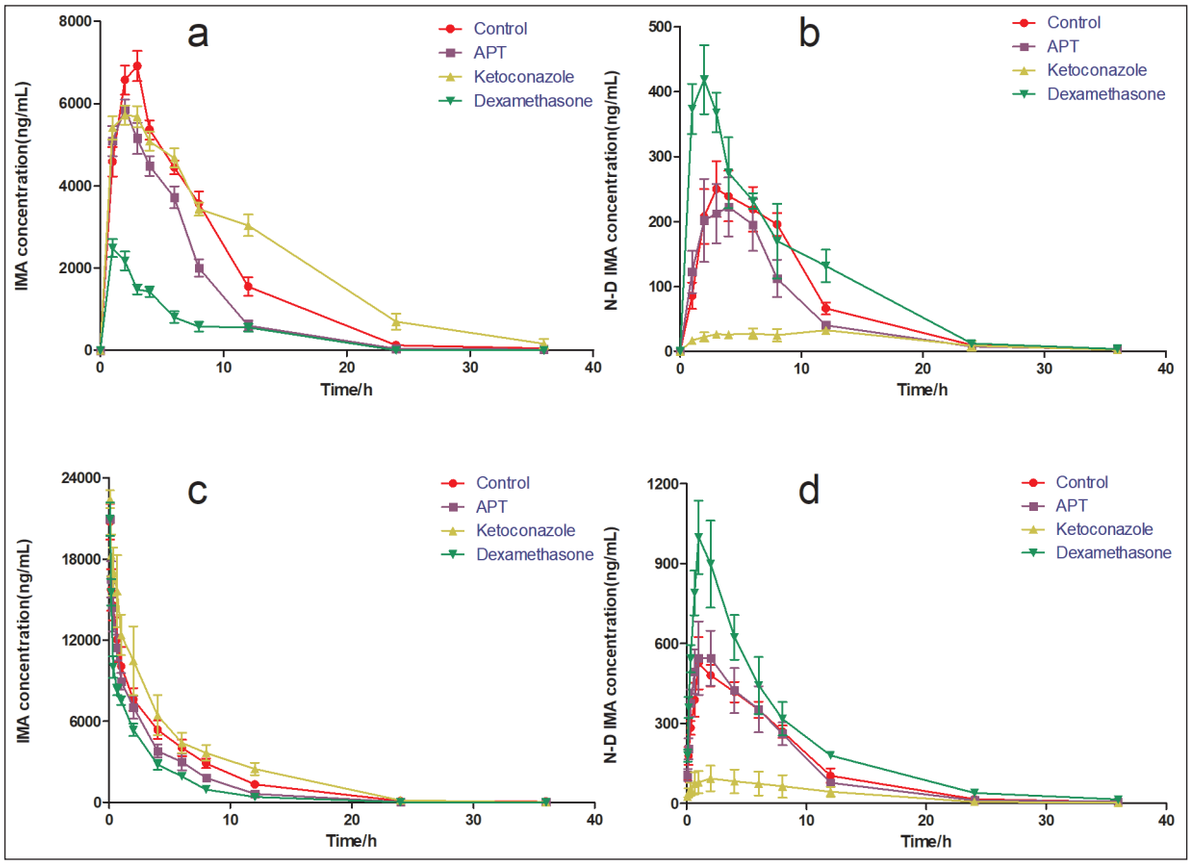

Fig. 2: Plasma concentration–time curves of IMA(a), N-D IMA (b) after orally given IMA and IMA(c), N-D IMA (d) after intravenously given IMA preadministered rats by oral CMC-Na (control), ketoconazole (inhibitor), dexamethasone (inducer) and APT (mean ± SD, n=6).

Table 2: Pharmacokinetic parameters of IAM and N-D IMA after intravenous administration of IMA (30 mg/kg) to the pretreated groups given oral 0.5% CMC-Na, ketoconazole (80 mg/kg) , dexamethasone- and (80 mg/kg) and APT (10 mg/kg) to rats for 3 consecutive days (n = 6)

Parameter	*Control*	*APT*	*Ketoconazole*	*Dexamethasone*
IMA				
$AUC_{0\text{-}t}$(mg·h·L^{-1})	70.51±9.22	53.35±7.34*	93.35±19.33*	38.81±3.5*
$AUC_{0\text{-}}$ (mg·h·L^{-1})	70.58±9.23	53.36±7.35*	93.82±19.7*	38.8±3.5*
$t_{1/2}$(h)	3.57±0.40	2.61±0.14	3.94±0.35	2.39±0.22
Vd(L·kg^{-1})	2.22±0.43	2.15±0.29	1.84±0.65	2.66±0.36
CL(L·h^{-1}·kg^{-})	0.43±0.06	0.57±0.07*	0.33±0.08*	0.77±0.03*
MRT(0-t)(h)	5.20±0.58	3.96±0.32*	5.66±0.39*	3.45±0.32*
MRT(0-∞)(h)	5.24±0.59	3.97±0.32*	5.83±0.65*	3.45±0.32*
N-D IMA				
$AUC_{0\text{-}t}$(mg·h·L^{-1})	4.71±0.62	4.62±0.94	1.20±0.70**	7.74±0.67**
$AUC_{0\text{-}}$ (mg·h·L^{-1})	4.74±0.64	4.63±0.94	1.22±0.70**	7.86±0.67**
Cmax(ug/L)	539.8±113.6	583.4±128.6	94.12±56.34**	998.7±235.6**
Tmax(h)	1.22±0.45	1.27±0.72	2±0.10	1.3±0.52
$t_{1/2}$(h)	4.77±1.20	3.80±0.18	5.99±1.25	6.33±0.69
Vd(L·kg^{-1})	43.84±11.30	36.57±6.62	292.3±176.0**	35.11±5.56*
CL(L·h^{-1}·kg^{-1})	6.42±0.90	6.68±1.30	31.55±15.25**	3.84±0.33*
MRT(0-t)(h)	6.75±0.57	6.20±0.40	8.64±0.82**	7.18±0.49*
MRT(0-∞)(h)	6.97±0.69	6.25±0.41	9.32±1.13**	7.78±0.52*

Each value represents the mean ± S.D. of six rats.
* Significantly different with P < 0.05 versus 0.5% CMC-Na (control group).
** Significantly different with P < 0.01 versus 0.5% CMC-Na (control group).

2.3. RT-PCR analysis of Cyp3a1, Abcg2 and Abcb1 mRNA in rat liver

Figure 3 shows the effect of APT on the expression levels of CYP3A1, Bcrp and Abcb1 in rat liver upon pretreatment with APT for 3 days. Compared to the control group (0.5% CMC-Na), the CYP3A1 level was increased (p<0.05) in the dexamethasone treated group, and CAP3A1 level was decreased (p<0.05) in the ketoconazole treated group, Abcg2 and Abcb1 were not significantly changed (P>*0.05*). However, CYP3A1 and P-gp levels in APT treated groups were all significantly increased (*P*<0.05), while Abcg2 was not significantly changed(P>*0.05*).

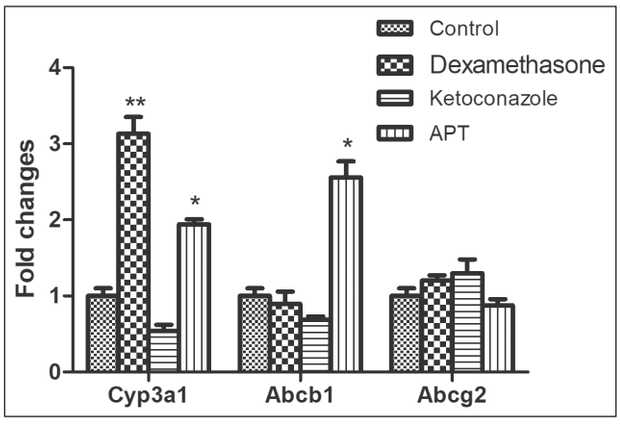

Fig. 3: Effect of APT treatment on mRNA expression of rat Cyp3a1, Abcb1 and Abcg2 in the liver following a 3-day treatment with 0.5% CMC-Na (control), ketoconazole (80 mg/kg), dexamethasone (80 mg/kg) and APT (10 mg/ kg) (n = 6). * Significantly different with P< 0.05 versus parameters of control group (0.5% CMC-Na).

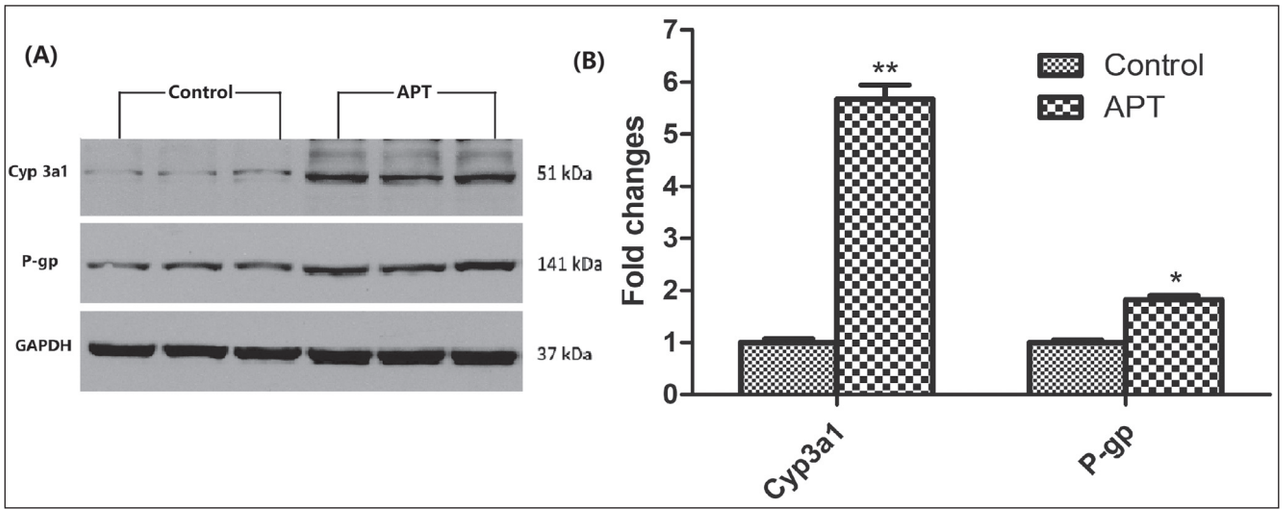

Fig. 4: Effect of APT once daily for 3 days at the dose of 10 mg kg^{-1} on protein expression of liver Cyp3a1 and P-gp in rats. a) An image of Western Blotting results; b) Analytical chart of Western Blotting results. * Significantly different with P< 0.05 versus parameters of control group (0.5% CMC-Na).

2.4. Western blotting analysis of CYP3A1 and P-gp in rat liver

CYP3A1 and P-gp expression levels were determined using GAPDH, anti-CYP3A1 and anti-Pgp in rat liver samples. APT significantly upregulated the CYP3A1 and P-gp expression levels once daily over three days pretreatment at 10 mg/kg. In Fig. 4, the bar graph shows quantification of band intensity; high bands intensity of CYP3A1 and Pgp proteins in APT treated group, stand for the significant inducing effect of APT on these proteins, equivalent to 5.67 and 1.82-fold (P<0.05) increase versus the control group (0.5% CMC-Na).

3. Discussion

In the pharmacokinetic study, ketoconazole and dexamethasone as CYP3A4 inhibitor and inducer, respectively, both significantly changed the bioavailability of IMA and its main metabolite N-D IMA. As expected, after the IMA was orally given to the rats, dexamethasone significantly decreased AUC, t1/2, Cmax of IMA and increased AUC, t1/2, Cmax of N-D IMA. Meanwhile, ketoconazole significantly increased AUC and t1/2 of IMA, but Cmax remained unchanged which indicated ketoconazole would impact the absorption speed and metabolism simultaneously and decrease AUC, Cmax of N-D IMA. When IMA was administered intravenously, AUC and MRT were decreased by more than 1.50-fold for IMA and increased by 1.64 and 1.06-fold for N-D IMA in the group pretreated with dexamethasone. Simultaneously, in the group pretreated with ketoconazole, AUC and MRT of IMA were increased. In contrast AUC and MRT of N-D IMA were decreased by more than 2.08-fold.

APT showed to be a moderate CYP3A4 inhibitor, which is consistent with in vitro data (Aapro and Walko 2010; Majumdar et al. 2003). Interestingly, Shadle et al. (2004) applied an aprepitant 3-day regimen (aprepitant 125 mg p.o. on day 1 and aprepitant 80 mg p.o. on days 2 and 3) or matching placebo in 24 healthy subjects. Assessed using intravenous midazolam as a probe, aprepitant 125/80 mg p.o. administered over days 1 to 3 produced a clinically insignificant weak inhibition (day 4) and induction (day 8) of CYP3A4 activity and no effect on CYP3A4 activity on day 15. In our experiment, we proposed an oral IMA and pretreatment 3 days APT interaction at first. Then, by intravenous injection of IMA, we ruled out the effect of intestinal absorption on IMA bioavailability. The result indicated that when IMA was administered orally or intravenously to rats after ingestion of APT for three days, the pharmacokinetic results revealed that the CL/F of IMA increased (P<0.05) by 1.4 and 1.3-fold respectively. Besides, there were 30.0 % (P<0.05) and 24.4% (P<0.05) reduction in the AUC(0-∞) of IMA compared to the control group after administration of oral and intravenous IMA (30 mg/kg). This implied that absorption did not affect IMA pharmacokinetics and the APT decreased bioavailability of IMA. Interestingly, N-D IMA as IMA metabolite showed just a slight decline of AUC, which was not statistically significant after oral administration of IMA. When the IMA was administered intravenously, the bioavailability of N-D IMA remained unchanged compared with the control group. This might imply that APT not only regulates CYP3A1, but also has another underlying mechanism which affects the metabolism of N-D IMA and even IMA. This is very likely a complex drug-drug interaction.

IMA is metabolized primarily to N-D IMA by CYP3A4 which is one of the rate-limiting steps in metabolism (Gotta et al. 2014; O'Brien et al. 2003). CYP3A4 modulators could alter IMA and its metabolite pharmacokinetic profiles and their responses at their sites of action which may lead to toxicity, resistance or treatment failure (Scripture et al. 2005). According to IMA pharmacokinetics in vivo, strong CYP3A4 inhibitors and inducers have obviously an effect (Wang et al. 2015). Moreover, there were not any studies reporting that APT exhibited inhibitory or inducing effects on CYP2C8. In spite of reports showing that CYP2C8 also plays an important role in chronic use of imatinib results in reduced CYP3A4 and CYP3A5 activity through autoinhibition (Filppula et al. 2013; Verboom et al. 2017). It was suggested that APT could not affect CYP2C8-mediated metabolism in APT-IMA interaction. Imatinib was initially determined to be a substrate for ABCB1 (P-glycoprotein) in vitro and in vivo (Dai et al. 2003; Hamada et al. 2003). Subsequently, it was demonstrated that imatinib was an inhibitor (Houghton et al. 2004) and substrate (Burger et al. 2004) of ABCG2 (BCRP). P-gp, an efflux protein located in the gastrointestinal tract, placenta, kidneys, brain, and liver, may also be involved in this process. The breast cancer resistance protein (BCRP), formally known as ATP-binding cassette protein G2 (ABCG2), is an efflux transporter that plays a significant role in altering absorption, distribution, metabolism, and excretion (ADME) of most extant and emerging molecular cancer therapeutics (Natarajan et al. 2012). Mlejnek et al. (2011) suggested that the intracellular level of N-D IMA was significantly lower than that of imatinib in K562/Dox cells, which represent a multidrug-resistant variant of K562 cells due to Pgp overexpression (Mlejnek et al. 2011). By considering our results in vivo, an assumption is that APT induced CYP3A1, P-gp, Bcrp level and accelerated IMA elimination. As a result, the efflux transporters modulation such as Bcrp or P-gp would lead to unchanged systemic exposure of N-D IMA which is supposed to be increased by CYP3A1 induction in the APT treated group.

For further study, we employed RT-PCR and western blotting to assess the changes of CYP3A1, P-gp and Bcrp in mRNA and

protein levels. The data confirmed that the mRNA expression levels of CYP3A1 and P-gp were increased (P< 0.05) in the liver of rats consuming APT compared to controls, but Bcrp was not significantly changed (P> 0.05). The increase in CYP3A1 and P-gp gene expression was consistent with the results obtained from western blotting in which APT induced CYP3A1 and P-gp protein expression. Based on the results, the expressions of P-gp and CYP3A1 were induced by APT. To determine the responsibility for the pharmacokinetics change of IMA and N-D IMA after pretreated with APT (10 mg/kg) for three days, the disposition of IMA in rat and APT concentration in plasma should be determined. In summary, APT could decrease the bioavailability of IMA in rats at daily doses of 10.0 mg/kg and P-gp and CYP3A1 in the liver were raised at both the mRNA and protein levels. These findings proved that ingestion of APT upregulated the expression of P-gp in rat liver, following by downregulation of N-D IMA exposure in rats. Consequently, since the elimination of the drug was altered when APT was co-administered to rats, the possibility of metabolic interactions between APT and IMA that are the mutual substrates of CYP3A1 enzyme and P-gp transporter must be considered.

4. Experimental

4.1. Chemicals and reagents

Imatinib mesylate, N-desmethyl imatinib ,aprepitant and gefitinib (internal standard, IS) were purchased from Dalian Meilun Biotech Co.,Ltd (Dalian, China). HPLC–grade methanol was obtained from Tedia (Tedia, fairfield, OH, USA). Formic acid was purchased from Aladdin industrial corporations (Shanghai, China). The water used for HPLC–MS/MS was purified by use of Milli–Q purification system (Millipore, Milford, MA, USA). All other chemicals were of analytical grades and were commercially available.

4.2. Animal experiments

Sprague–Dawley (SD) male rats of 180 – 220 g were obtained from the Animal Center of Tongji Medical College of Huazhong University of Science and Technology (Wuhan, Hubei, China). Rats were randomly divided into four groups by means of 6 rats in each cage (n=6), through food and water free accessibility in a temperature (25 °C) and 12 h night/12 h day rhythm controlled room.

The rats were randomly divided into eight groups: (1A, 1B) control group (prereated with 0.5% CMC-Na, p.o., n=6, respectively); (2A, 2B) APT group (pretreated with APT in 0.5% CMC-Na, 10 mg/kg, p.o., n=6, respectively); (3A, 3B) inhibition group (pretreated with ketoconazole in 0.5% CMC-Na, 80 mg/kg, p.o., n=6, respectively); (4A, 4B) induction group (pretreated with dexamethasone in 0.5% CMC-Na, 80 mg/kg, p.o., n=6, respectively). All the rats were given vehicle (control group) or drug (other groups) daily by gastrogavage for 2 days. twelve hours after the last treatment with APT, access to the diet was removed and only water was provided. On the 3rd day, rats were treated with vehicle or drug. 30 min after treatment, IMA (30 mg/kg, dissolved in 0.5% CMC-Na) was administered to rats in A groups (1A, 2A, 3A and 4A group). After administration, 300 µl retro-orbital blood samples were collected at a series of time points (1, 2, 3, 4, 6, 8, 12, 24, 36 h) in heparinized tubes. Meanwhile, the rats in B group (1B, 2B, 3B and 4B group) were injected through the lateral tail vein by IMA (30 mg/kg, dissolved in 5% glucose solution) 30 min after the last pretreatment. 300 µl blood samples were collected at predose, 5, 10, 20, 40 min and 1, 2, 4, 6, 8, 12 , 24 and 36 h. All the blood samples were vortexed and centrifuged at 3000 rpm, 4 °C for 10 min. The rats were sacrificed after the last point of blood collection. The liver samples were removed and all stored immediately at -80 °C until analysis. All the experimental works were performed to meet the requirements by the Animal Care Committee of Huazhong University of Science and Technology.

4.3. Apparatus

Analysis was performed on Waters ACQUITY Ultra performance liquid chromatography system (Waters, USA) equipped with an online degasser, a quaternary pump, an autosampler and an autosampler thermostat. API 4000+ LC–MS/MS System (AB SCIEX, American) equipped with Turbo positive electrospray ionization (ESI) and multiple reaction monitoring (MRM) modes was used for detection. Data acquisition was carried out using Analyst 1.6.1 software (AB SCIEX).

4.4. Analytical methods

A 550 µL aliquot of methanol containing 10 µL of IS (1 µg/mL) was used for liquid-liquid extraction of 50 µL plasma sample. The resulting supernatant was collected for injection after the mixtures vortexed for 3 min and centrifuged for 10 min at 14,000 rpm. Chromatographic separation was carried out, using isocratic elution with water and methanol containing 0.1% formic acid (45:55, v/v) on a Welch Ultimate XB-C18 column (5 µm, 2.1×100 mm, Shanghai, China) with the flow rate of 0.3 mL/min and the injection volume of 5 µL under 40 °C of column temperature. The optimal condition consisted of the collision–activated dissociation (CAD) gas, a curtain gas (CUR), a nebulizer gas (GS1), a Turbo Ion Spray gas (GS2) of 8, 25, 55 and 55 psi respectively. The ion spray voltage and a source temperature were 5500 V and 550 °C relatively. The mass charge ratio (m/z) of the precursor-product ion pairs were 494.20→394.3 for IMA, 480.3→394.3 for N-D IMA and 447,1→128.6 for gefitinib emerged on the most intense mass spectra. The total analytical run of each sample was 3.5 min.

4.5. Pharmacokinetic and statistical analysis

Non compartmental pharmacokinetic model of analysis was implemented for this study and the results are given as mean±standard deviation (SD). The Drug and Statistics (DAS) 3.2.8 software was used to calculate the subsequent parameters: The geometric mean area under the plasma concentration–time curve from time 0 to the last measurable time and from time 0 to infinity for AUC_{0-t} and $AUC_{0-\infty}$ respectively. Half-life ($t_{1/2}$), Mean residence time (MRT), apparent total clearance (CL/F) and apparent volume of distribution (V/F) obtained from AUC values. Peak plasma concentration (C_{max}) and time to reach C_{max} (t_{max}) obtained directly from the observed data. The above parameters for IMA and N-D IMA in each group were compared to control group using SPSS version 16.0 (one-way ANOVA test) to find significance of variation. The analysis was completed by Graph Pad Prism 5.01 software (San Diego, CA).

4.5. Reverse transcriptase-polymerase chain reaction (RT-PCR) assay

RNA was extracted from liver samples using the RNAiso Plus (TaKaRa Biotechnology, Dalian, China, Cat.#D9108) following the manufacturer´s instructions and then reversely transcribed to cDNA using PrimeScriptTM RT reagent kit with gDNA Eraser (TaKaRa Biotechnology, Cat. #RR036A). The RT-PCR was carried out to determine the level of Cyp3a1, Abcg2 and Abcb1 mRNA expression by using SYBR® Premix ExTaqTM (TaKaRa Biotechnology, Cat.#RR420A) in a 20 µL reaction system. The reaction system contained 2 µL of cDNA, 10 µL of SYBR Premix Ex TaqTM and 0.2 µM each of the forward and reverse primers (Table 3). The samples were initially denatured at 95 °C for 30 s and amplified using 40 cycles of 95 °C for 5 s, 60 °C for 30 s and dissociated at 95 °C for 15 s, 60 °C for 60 s, 95 °C for 15 s on a StepOnePlus RT-PCR System (Life Technologies, Carlsbad, CA). Primers used in this study were designed and synthesized by TaKaRa. GAPDH was used as an internal control.

Table 3: PCR primers for Abcb1, $CYP3_{A1}$, Abcg2and GAPDH

GENE	Primers(5'-3')	Product Size(bp)	Genbank number
Abcb1	F:TTCGGGATGTTTCGCTAT R:GGATGTAGGCAACGATGAG	286	NC_005103.4
Cyp3a1	F:CCTCTGTTTGCCATCACG R:AACACTTCTTTCACAGGGAC	284	NC_005111.4
Abcg2	F:AGAGTGGCTTTCTAGTCCG R:AATTGGCAGGTTGAGGTG	201	NC_005103.4
GAPDH	F:CATCACCATCTTCCAGGAGCGAGA R:TGCAGGATGCATTGCTGACAATCT	239	NC_005103.4

4.6. Western blotting assay

Total protein was prepared by homogenizing the liver samples in 10 volumes of RIPA Lysis Buffer (ASPEN, Hubei, China). The tube was submersed in a small bucket of ice and water during all homogenization, followed by centrifugation (12000 rpm) for 5 min. The supernatant was the total protein of livers. Protein concentrations were measured using a BCA Protein Assay Kit (Goodbio, Hubei, China) according to the manufacturer's instructions. Western Blotting for the immunodetection of CYP3A1 was obtained using 40 µg of extracted membrane proteins in loading buffer (0.25 M Tris base pH 6.8, 50% glycerol, 10% SDS, 0.5% bromophenol blue and 5% mercaptoethanol). Protein samples were subject to SDS-polyacrylamide gel electrophoresison 10 %polyacrylamide gel at 120 V for 2 h and transferred onto a PVDF membrane. The membrane was blocked by incubating for 1 h at room temperature with Tris buffered saline containing 0.1% Tween 20 and 5% dried skim milk, then incubated with the anti-CYP3A1, anti-Pgp monoclonal antibody C219 (Calbiochem,

Gibbstown, NJ) and anti-GAPDH (santa, Shanghai, China) overnight at 4 °C. The membrane was washed (4.5 min), incubated with secondary antibody (KPL, Beijing, China) horseradish peroxidase conjugate (1:10000) for 30 min, and washed again (4.5 min). The protein of interest was detected with enhanced chemiluminescence substrate (Millipore) and imaged using a Kodak film.

Acknowledgements: This study was financially supported by the National Natural Science Foundation of China (grants# 81473287, 81673715, and 81403012).

Conflict of interest: The authors declare that there are no conflicts of interest.

Ethical approval: The study was approved by the local Animal Ethic Committee.

References

Aapro MS, Walko CM (2010) Aprepitant: drug-drug interactions in perspective. Ann Oncol 21: 2316-2323.

Burger H, Van TH, Boersma AW, Brok M, Wiemer EA, Stoter G, Nooter K (2004) Imatinib mesylate (STI571) is a substrate for the breast cancer resistance protein (BCRP)/ABCG2 drug pump. Blood 104: 2940-2942.

Dai H, Marbach P, Lemaire M, Hayes M, Elmquist WF (2003) Distribution of STI-571 to the brain is limited by P-glycoprotein-mediated efflux. J Pharmacol Exp Ther 304: 1085-1092.

Delbaldo C, Chatelut E, Ré M, Deroussent A, Séronievivien S, Jambu A, Berthaud P, Le CA, Blay JY, Vassal G (2006) Pharmacokinetic-pharmacodynamic relationships of imatinib and its main metabolite in patients with advanced gastrointestinal stromal tumors. Clin Cancer Res 12: 6073-6078.

Depré M, Van HA, Oeyen M, De LI, Laethem T, Rothenberg P, Petty KJ, Majumdar A, Crumley T, Panebianco D (2005) Effect of aprepitant on the pharmacokinetics and pharmacodynamics of warfarin. Eur J Clin Pharmacol 61: 341-346.

Egerer G, Eisenlohr K, Gronkowski M, Burhenne J, Riedel KD, Mikus G (2010) The NK1 receptor antagonist aprepitant does not alter the pharmacokinetics of high-dose melphalan chemotherapy in patients with multiple myeloma. Brit J Clin Pharmacol 70: 903-907.

Feuring M, Lee Y, Orlowski LH, Michiels N, De Smet M, Majumdar AK, Petty KJ, Goldberg MR, Murphy MG, Gottesdiener KM, Hesney M, Brackett LE, Wehling M (2003) Lack of effect of aprepitant on digoxin pharmacokinetics in healthy subjects. J Clin Pharmacol 43: 912-917.

Filppula AM, Neuvonen M, Laitila J, Neuvonen PJ, Backman JT (2013) Autoinhibition of CYP3A4 leads to important role of CYP2C8 in imatinib metabolism: variability in CYP2C8 activity may alter plasma concentrations and response. Drug Metabol Dispos 41: 50-59.

Fujiwara Y, Toyoda M, Chayahara N, Kiyota N, Shimada T, Imamura Y, Mukohara T, Minami H (2014) Effects of aprepitant on the pharmacokinetics of controlled-release oral oxycodone in cancer patients. Plos One 9: e104215.

George S, Trent JC (2011) The role of imatinib plasma level testing in gastrointestinal stromal tumor. Cancer Chemother Pharm 67: 45-50.

Gotta V, Widmer N, Decosterd LA, Chalandon Y, Heim D, Gregor M, Benz R, Leoncinifranscini L, Baerlocher GM, Duchosal MA (2014) Clinical usefulness of therapeutic concentration monitoring for imatinib dosage individualization: results from a randomized controlled trial. Cancer Chemother Pharmacol 74: 1307-1319.

Hamada A, Miyano H, Watanabe H, Saito H (2003) Interaction of imatinib mesilate with human P-glycoprotein. J Pharmacol Exp Ther 307: 824-828.

Houghton PJ, Germain GS, Harwood FC, Schuetz JD, Stewart CF, Buchdunger E, Traxler P (2004) Imatinib mesylate is a potent inhibitor of the ABCG2 (BCRP) transporter and reverses resistance to topotecan and SN-38 in vitro. Cancer Res 64: 2333-2337.

Huskey SE, Dean BJ, Doss GA, Wang Z, Hop CE, Anari R, Finke PE, Robichaud AJ, Zhang M, Wang B, Strauss JR, Cunningham PK, Feeney WP, Franklin RB, Baillie TA, Chiu SH. (2004) The metabolic disposition of aprepitant, a substance P receptor antagonist, in rats and dogs. Drug Metab Dispos 32: 246-258.

Khan MS, Barratt DT, Somogyi AA (2016) Impact of CYP2C8*3 polymorphism on in vitro metabolism of imatinib to N-desmethyl imatinib. Xenobiotica 46: 278-287.

Majumdar AK, Mccrea JB, Panebianco DL, Hesney M, Dru J, Constanzer M, Goldberg MR, Murphy G, Gottesdiener KM, Lines CR (2003) Effects of aprepitant on cytochrome P450 3A4 activity using midazolam as a probe. Clin Pharmacol Ther 74: 150-156.

Mlejnek P, Dolezel P, Faber E, Kosztyu P (2011) Interactions of N -desmethyl imatinib, an active metabolite of imatinib, with P-glycoprotein in human leukemia cells. Ann Hematol 90: 837-842.

Natarajan K, Xie Y, Baer MR, Ross DD (2012) Role of breast cancer resistance protein (BCRP/ABCG2) in cancer drug resistance. Biochem Pharmacol 83: 1084-1103.

O'Brien SG, Meinhardt P, Bond E, Beck J, Peng B, Dutreix C, Mehring G, Milosavljev S, Huber C, Capdeville R (2003) Effects of imatinib mesylate (STI571, Glivec) on the pharmacokinetics of simvastatin, a cytochrome P450 3A4 substrate, in patients with chronic myeloid leukaemia. Brit J Cancer 89: 1855-1859.

Prueksaritanont T, Chu X, Gibson C, Cui D, Yee KL, Ballard J, Cabalu T, Hochman J (2013) Drug-drug interaction studies: regulatory guidance and an industry perspective. AAPS J 15: 629-645.

Rochat B, Zoete V, Grosdidier A, Von GS, Marull M, Michielin O (2010) In vitro biotransformation of imatinib by the tumor expressed CYP1A1 and CYP1B1. Biopharm Drug Dispos 29: 103-118.

Scripture CD, Sparreboom A, Figg WD (2005) Modulation of cytochrome P450 activity: implications for cancer therapy. Lancet Oncol 6: 780-789.

Shadle CR, Lee Y, Majumdar AK, Petty KJ, Gargano C, Bradstreet TE, Evans JK, Blum RA (2004) Evaluation of potential inductive effects of aprepitant on cytochrome P450 3A4 and 2C9 activity. J Clin Pharmacol 44: 215-223.

Takahashi N, Miura M (2012) Therapeutic drug monitoring of imatinib for chronic myeloid leukemia patients in the chronic phase. Pharmacology 87: 241-248.

Verboom MC, Visser L, Kouwen S, Swen JJ, Diepstraten J, Posthuma WF, Gelderblom H, Van LD, Wilms EB (2017) Influence of CYP2C8 polymorphisms on imatinib steady-state trough level in chronic myeloid leukemia and gastrointestinal stromal tumor patients. Pharmacogenet Genomomics 27: 223-226.

Wang Z, Wang L, Xia MM, Sun W, Huang CK, Cui X, Hu GX, Lian QQ, Wang ZS (2015) Pharmacokinetics interaction between imatinib and genistein in rats. Biomed Res Int 2015: 368976.

Zitvogel L, Rusakiewicz S, Routy B, Ayyoub M, Kroemer G (2016) Immunological off-target effects of imatinib. Nat Rev Clin Oncol 13: 431-446.